

Article

Methods for Measuring and Assessing Irregularities of Stone Pavements—Part II

Giuseppe Cantisani ^{*}, Salvatore Bruno , Antonio D'Andrea , Giuseppe Loprencipe , Paola Di Mascio 
and Laura Moretti ¹

Department of Civil, Constructional and Environmental Engineering, Sapienza University of Rome,
Via Eudossiana 18, 00184 Rome, Italy

* Correspondence: giuseppe.cantisani@uniroma1.it; Tel.: +39-064-458-5117

Abstract: This two-part manuscript presents a comprehensive methodology for the irregularity assessment of urban stone pavements. The proper road surface assessment using key performance indicators is necessary to plan appropriate maintenance strategies. However, there are no monitoring methods or evaluation criteria for stone pavements whose surfaces are more uneven than traditional ones due to their structural characteristics. Therefore, it is useful to define criteria for assessing irregularities considering the comfort experienced by road users and classify their conditions. This second part presents the geometric and comfort analyses of 40 urban branch profiles to describe pavement unevenness. In particular, four methods have been investigated: the International Roughness Index (IRI) according to ASTM E1926, the surface profile classification according to ISO 8608, the comfort index (a_{wz}) according to ISO 2631, and the straightedge analysis for stone pavements (SASP) proposed by the authors that is able to evaluate the effect of localized irregularities, taking into account different urban vehicles. In conclusion, four classes have been defined to describe geometric and comfort conditions that can support road manager decisions in order to implement an effective pavement management system.

Keywords: stone pavements; pavement roughness; assessment methods; urban road safety; vulnerable road users; user riding comfort



check for updates

Citation: Cantisani, G.; Bruno, S.; D'Andrea, A.; Loprencipe, G.; Di Mascio, P.; Moretti, L. Methods for Measuring and Assessing Irregularities of Stone

Pavements—Part II. *Sustainability* **2023**, *15*, 3715. <https://doi.org/10.3390/su15043715>

Academic Editors: Rosolino Vaiana and Vincenzo Gallelli

Received: 29 November 2022

Revised: 8 February 2023

Accepted: 15 February 2023

Published: 17 February 2023



Copyright: © 2023 by the authors. Licensee MDPI, Basel, Switzerland. This article is an open access article distributed under the terms and conditions of the Creative Commons Attribution (CC BY) license (<https://creativecommons.org/licenses/by/4.0/>).

1. Introduction

Historical stone pavements were not designed to accommodate the modern traffic categories and should balance often conflicting goals of safety [1], comfort, low impact [2], low maintenance [3], and low cost [4,5]. In the literature, functional criteria to analyze [6,7] and manage block pavements have rarely been investigated [8,9]. However, it would be useful to identify roughness and manage these surfaces according to the expected traffic categories (e.g., pedestrians, two-wheeled vehicles, light vehicles, heavy vehicles, or buses). Measurements or surveys with static or dynamic monitoring instruments give information about the surface performances [10]. In fact, it should be considered that circulation on these pavements can cause disturbing effects on the surrounding environment due to rolling noise and vibrations. Regarding this aspect, for example, Garilli et al. [11] proposed a method for evaluating the functional and safety performances of stone pavements, taking into account pedestrians with wheeled trolleys.

Then, it is necessary to define criteria for evaluating the stone pavements by providing the range of variability for the adopted indices and the expected operating conditions. The overall decision-making process helps road managers to identify priorities and schedule maintenance [12] based on a Pavement Management System (PMS).

In this study, both traditional and innovative methods to evaluate surface and riding conditions have been applied to different road pavements. Profilometric measurements were carried out on 34 stone pavements, 2 concrete block pavements, 3 asphalt concrete

(AC) pavements with different levels of distress, and one unpaved road for a total of 40 surfaces. Indeed, the profiles have been investigated with different methods to assess the International Roughness Index, carry out the classification according to ISO 8608 [13], assess the riding comfort level according to ISO 2631 [14], and analyze the profiles in terms of bump length (*BL*) and bump height (*BH*) inspired by the method adopted for airfield pavement roughness in the FAA procedure [15]. The first three methods are not designed for stone pavements and do not distinguish between localized and distributed defects that affect the riding quality. Moreover, they are not specialized to consider road users differing in speed and vehicles with different pitch. Then, in the absence of proper methods to collect and thresholds to interpret data profiles, the authors proposed a methodology to overcome the limitations of these methods and identify thresholds for modular pavements in urban areas [16]. It is based on the geometrical analysis of pavement profiles with a straightedge [15] whose length depends on the reference vehicle. It permits the calculation of the maximum amplitude of irregularities present in the pavement for several wavelengths [17]. Given the comfort results from the implementation of ISO 2631 [14,18–26], threshold curves have been proposed by the authors to classify the irregularities of the surveyed stone pavements varying the reference vehicle (i.e., bicycle, automobile, and bus). The results quantify surface defects and support road manager decisions to implement a pavement management system.

2. Materials and Methods

The aim of this research was to define the criteria for evaluating the roughness conditions of stone paving with reference to the comfort experienced by users, considering different vehicles. With this aim, a set of block paving was considered, characterized by different levels of unevenness. These levels were assessed by profilometric measurements using the KPIs currently in use. It was immediately clear that these KPIs are not adequate to classify modular paving because the KPIs always exceed the thresholds defined for the so-called even pavements.

In order to assess the irregularities with the methods proposed in the previous sections for the stone pavements and to define the criteria for evaluating the traffic conditions relating to users' comfort for the vehicles considered, a heterogeneous sample of pavements were measured with a contact profilometer type Dipstick[®] 2277 [27].

The choice of this Class I device made it possible to obtain measurements with a high degree of precision and accuracy (better than 0.0127 mm) and the measurements resulted in overcoming problems of interaction with traffic as almost all roads were subject to limited traffic. It was decided to measure profiles with a length of 80 m with a sampling step of 25 cm for a total of 321 measurements; this length was a fair compromise with respect to the operational needs and the road branch lengths. The time to acquire a profile was about 10 min for each segment. Normally, given that most surveyed roads were one-way and with reduced width, to limit traffic disturbance, only one profile was detected for each road section. Only where the traffic conditions allowed it, two profiles (one for each wheel path) were detected to take into account the roll motions in the three-dimensional models.

In the sections where it was not possible to measure two different pavement profiles, the same profile was used for both wheel paths in the simulations with the three-dimensional mechanical models.

In total, 58 profiles were detected to characterize 40 road branches in order to verify the practicability conditions. In addition to various types of stone pavements, the pavement profiles in concrete blocks subjected to vehicular and pedestrian traffic were measured (for a total of 54 modular pavement profiles, of which 52 were natural stone).

Figure 1 show the main characteristics of the considered pavements.



Figure 1. Images of the pavement types considered in this study.

The authors studied the collected branch profiles with the methods discussed in the first part of this paper:

- International Roughness Index (IRI) is a geometric method to evaluate the condition of paved surfaces [28]. However, limitations concern the reference speed (i.e., 80 km/h); the types of assessed defects, because IRI performs badly in interpreting isolated and localized defects; and the threshold values available in the literature, because data do not refer to modular pavements.
- Classification according to ISO 8608 [13] is a geometric method that provides a synthetic description of the road pavement surface. It classifies road profiles in terms of Power Spectral Density (PSD) but overlooks the vehicle type or the driving speed and does not properly consider the different vibration levels affecting road users.
- Comfort evaluation according to ISO 2631 [14] is based on the whole-body vibration perceived by users on-board a vehicle as a function of the longitudinal road roughness. The frequency-weighted vertical accelerations (a_{wz}) depend on the riding vehicle (or the vehicle mechanical model) and the vehicle speed [29]. This method allows comfort assessment for public transport [18–26]. In this paper three different dynamic vehicle models (i.e., bike, automobile, and bus) have been considered and discussed in the first part of this paper to investigate how vehicles affect the perceived comfort under different driving conditions.
- Straightedge analysis for stone pavements (SASP). It consists in the geometric analysis of the profile with respect to one or more reference lengths (straightedge) by calculating the maximum and average deviations as the straightedge position varies. Although this method is adopted for airfield pavement roughness in the FAA procedure [15], it has been adapted to urban stone pavements. It can evaluate the effects of both surface and localized irregularities on traffic. SASP permits the identification the location of the most severe punctual irregularities. Moreover, the authors proposed threshold curves that depend on the reference vehicle and allow both a relative comparison between surface irregularities and the classification of their functional performance.

3. Results

3.1. Geometric Methods: IRI and ISO 8608 Classification

Table 1 lists the IRI values and the ISO 8608 classification obtained for the 40 investigated branches (BR_i, with $i = 1, \dots, 40$). In particular, according to ISO 8608 the reference spatial frequency (n_0) and the waviness (w) have been considered. If available, both the right (rg) and left (lf) profile per each branch have been examined to identify IRI_{rg} and IRI_{lf}, n_{0_rg} and n_{0_lf} , and w_{rg} and w_{lf} , respectively.

Table 1. IRI and ISO 8608 classification.

Code	Type	Age (year)	IRI m/km	IRI _{lf} m/km	IRI _{rg} m/km	n_0 (cycles/m)		w		ISO 8608 Class
						n_{0_lf}	n_{0_rg}	w_{lf}	w_{rg}	
BR_1	1	>30	12.87	14.85	10.88	1538.5	662.2	-2.416	-2.254	D/D
BR_2	5	>100	16.26	15.40	17.11	1409.7	1124.2	-1.757	-1.366	D/D
BR_3	8	-	25.67	-	-	3933.7	-	-3.258	-	E
BR_4	7	5–10	5.42	4.89	5.94	174.4	142.6	-2.174	-2.169	C/C
BR_5	7	5–10	8.35	-	-	432.9	-	-2.482	-	C
BR_6	6	5–10	5.43	-	-	135.7	-	-2.104	-	C
BR_7	6	5–10	5.65	-	-	302.4	-	-2.982	-	C
BR_8	9	5–10	2.69	-	-	55.6	-	-1.821	-	B
BR_9	9	>10	11.47	-	-	280.2	-	-1.937	-	C
BR_10	9	>10	9.38	-	-	201.1	-	-1.350	-	C
BR_11	1	3–5	8.41	8.12	8.70	533.7	416.9	-2.156	-2.635	D/C
BR_12	3	>10	10.51	10.34	10.67	305.5	238.6	-1.727	-1.941	C/C
BR_13	1	>10	11.40	10.28	12.51	1042.7	621.2	-2.512	-2.426	D/D
BR_14	3	>20	20.10	19.80	20.39	2274.6	2119.8	-2.069	-2.768	E/E
BR_15	3	>10	13.08	12.95	13.20	1075.8	1191.9	-2.721	-2.696	D/D
BR_16	3	<5	14.85	14.81	14.88	255.2	306.0	-1.714	-2.049	C/C
BR_17	2	<5	7.74	7.64	7.84	138.1	139.6	-1.838	-1.795	C/C
BR_18	2	<5	6.52	6.79	6.24	140.7	218.8	-1.933	-1.860	C/C
BR_19	3	>10	13.87	14.64	13.09	689.9	1048.1	-1.755	-2.106	D/D
BR_20	1	>10	12.41	13.25	11.57	480.3	524.8	-2.019	-1.988	C/D
BR_21	3	>10	14.33	14.08	14.58	814.4	984.6	-1.953	-2.157	D/D
BR_22	3	>20	12.85	11.53	14.16	1427.3	802.1	-2.340	-2.068	D/D
BR_23	3	>20	13.62	13.63	13.61	986.8	1347.8	-2.006	-2.276	D/D
BR_24	3	>20	14.03	13.95	14.10	1439.8	1090.1	-2.600	-2.249	D/D
BR_25	1	>10	10.39	10.69	10.08	656.2	497.4	-2.376	-2.412	D/C
BR_26	6	>10	8.41	-	-	717.9	-	-2.098	-	D
BR_27	6	>10	6.56	-	-	316.6	-	-2.129	-	C
BR_28	1	<2	7.57	-	-	516.1	-	-2.541	-	D
BR_29	3	>20	16.62	-	-	2451.7	-	-2.753	-	E
BR_30	3	>20	18.13	-	-	1704.3	-	-2.252	-	D
BR_31	3	>20	15.27	-	-	1269.8	-	-2.350	-	D
BR_32	1	>10	9.71	-	-	456.9	-	-2.449	-	C
BR_33	3	>20	21.35	-	-	2595.6	-	-2.426	-	E
BR_34	3	>10	14.01	-	-	867.7	-	-2.189	-	D
BR_35	1	5–10	7.40	-	-	381.1	-	-2.457	-	C
BR_36	3	>20	18.93	-	-	3188.2	-	-2.828	-	E
BR_37	3	>20	15.97	-	-	1715.4	-	-2.346	-	D
BR_38	3	>20	17.99	-	-	2202.7	-	-2.789	-	E
BR_39	4	>10	11.74	-	-	1416.8	-	-2.884	-	D
BR_40	4	<2	9.99	-	-	342.7	-	-2.285	-	C

The Shapiro–Wilk normality test [30] on the IRI values of 54 block pavement profiles revealed the normal distribution of the population. Therefore, the mean and standard deviation values (i.e., $IRI_{avg} = 12.15$ m/km and $IRI_{SD} = 4.10$ m/km, respectively) allow the statistical interpretation of the sample. Figure 2 compares the results with the IRI distribution curve of AC surfaces considered in the previous study [31] ($IRI_{avg} = 2.11$ m/km and $IRI_{SD} = 1.18$ m/km). In this study, red bars are used for asphalt pavements and yellow bars for modular pavements. The two normal statistical distributions partially overlap each other, and the common area of the Gaussians is less than 5%. These results avoid using those IRI thresholds for block pavements which are valid for asphalt ones.

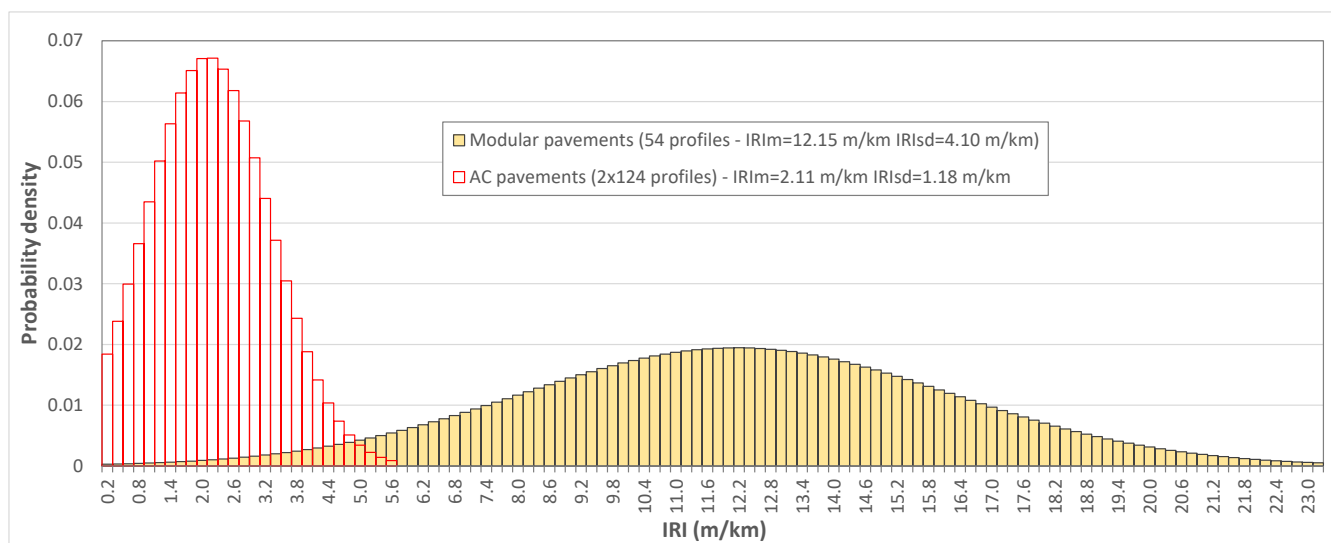


Figure 2. IRI Normal distributions of AC and modular pavements.

With regard to the entire dataset in Table 1,

- twenty class C profiles have n_0 values between 135.7 cycles/m and 497.4 cycles/m ($n_{0\text{avg}} = 291.1$ cycles/m), w values between -1.714 and -2.982 ($w_{\text{avg}} = -2.158$), and IRI values between 4.89 m/km and 14.88 m/km ($\text{IRI}_{\text{avg}} = 8.76$ m/km);
- twenty-eight class D profiles have n_0 values between 516.1 cycles/m and 1715.4 cycles/m ($n_{0\text{avg}} = 1043.6$ cycles/m), w values between -1.366 and -2.884 ($w_{\text{avg}} = -2.244$), and IRI values between 7.57 m/km and 18.13 m/km ($\text{IRI}_{\text{avg}} = 13.07$ m/km);
- six class E profiles have n_0 values between 2119.8 cycles/m and 3188.2 cycles/m ($n_{0\text{avg}} = 2472.1$ cycles/m), w values between -2.069 and -2.828 ($w_{\text{avg}} = -2.606$), and IRI values between m/km 16.62 and 21.35 m/km ($\text{IRI}_{\text{avg}} = 19.18$ m/km).

As for the range of IRI values associated with the ISO 8608 classes, the obtained data show that the profiles with IRI between 7.57 m/km and 14.88 m/km belong to C or D class depending on their frequency content. The trend of IRI values confirms the pavement irregularity increases from C to E class, the average value of n_0 increases as the class varies (i.e., from 291.1 cycles/m for C to 2472.1 cycles/m for E), while w decreases (i.e., from -2.158 for C to -2.606 for E). Figure 3 shows the classes' distribution according to ISO 8608 [32], that is, asymmetrical and centered on class D for the block pavements and on class B for the asphalt ones. With regard to the examined modular pavements, 63% fall into the worst classes (i.e., D and E). However, these results do not provide any information useful for road manager to schedule maintenance and/or restrict the circulation.

3.2. Comfort Evaluation According to ISO 2631

The ISO 8608 methodology embodies the frequency content of the profiles better than the IRI index, but only vehicle mechanical models can simulate the operating conditions to investigate the relationship between the frequency content and the effect on user comfort. For this reason, the authors simulated three vehicle models at different constant speed values that are typical for the surveyed urban branches:

- Bike model (5 dof) at 10 km/h and 20 km/h;
- Automobile model (8 dof) at 30 km/h and 50 km/h;
- Bus model (8 dof) at 30 km/h and 50 km/h.

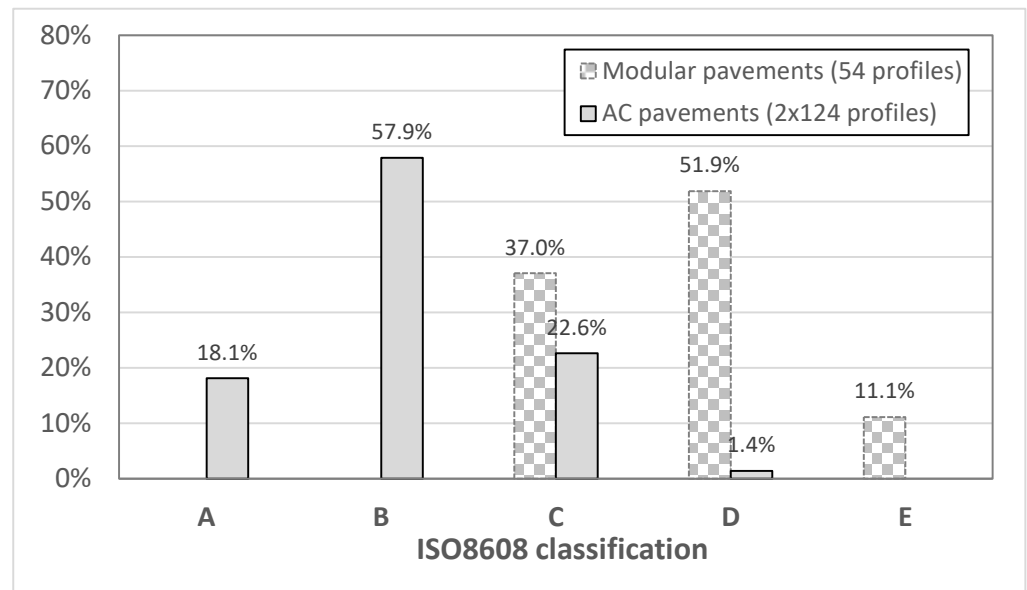


Figure 3. Distribution of ISO 8608 classification for asphalt and modular pavements.

For each vehicle, the authors proposed four comfort classes inspired by ISO 2631 varying the $a_{wz,S}$ thresholds (with S equal to the speed of the simulated vehicle in km/h). The proposed classes (i.e., Class 1 to 4) range from comfortable/little uncomfortable (i.e., Class 1) to uncomfortable/very uncomfortable (i.e., Class 4) riding conditions (Table 2).

Table 2. Proposed comfort classes.

	Bike Model (5 dof)		Automobile Model (8 dof)		Bus Model (8 dof)					
	$a_{wz,10}$ (m/s ²)	$a_{wz,20}$ (m/s ²)	$a_{wz,30}$ (m/s ²)	$a_{wz,50}$ (m/s ²)	$a_{wz,30}$ (m/s ²)					
Class 1 (Not uncomfortable/Little uncomfortable)	≤ 0.63	≤ 1.0	≤ 0.5	≤ 0.63	≤ 0.5					
Class 2 (Little uncomfortable/Fairly uncomfortable)	> 0.63	≤ 1.0	> 1.0	≤ 1.25	> 0.5	≤ 0.63	> 0.63	≤ 0.8	> 0.5	≤ 0.8
Class 3 (Fairly uncomfortable)	> 1.0	≤ 1.25	> 1.25	≤ 1.6	> 0.63	≤ 0.8	> 0.8	≤ 1.0	> 0.8	≤ 1.0
Class 4 (Uncomfortable/Very-Extremely uncomfortable)	> 1.25	> 1.6	> 0.8	> 1.0	> 1.0					

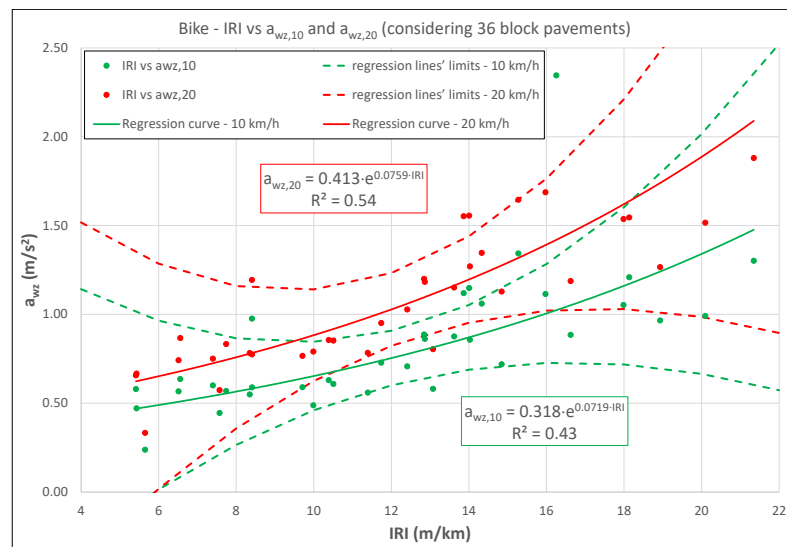
For the bus model, the simulations carried out at speeds of 50 km/h gave some a_{wz} values higher than 2.5 m/s² (extremely uncomfortable according to [14]), bold values in Table 3). These results have been neglected for the definition of the comfort classes, but they enabled us to identify extreme disturbance conditions for urban bus passengers when the vehicle moves at high speed on block pavements. Table 3 lists the a_{wz} values obtained for all the investigated branches using three simulation vehicle models with two speeds each; the colors in Table 3 comply with the chromatic notation of Table 2.

With regard to the modular pavements in Table 1, Figure 4a–c show interesting correlations (solid lines) between the IRI values in Table 1 and the a_{wz} values in Table 3 for bike, automobile, and bus models, respectively. High R² values (i.e., 0.84–0.85) demonstrate the correlation between IRI, $a_{wz,30}$, and $a_{wz,50}$ with the automobile model, and $a_{wz,30}$ with the bus model. On the other hand, low R² values (i.e., 0.43–0.63) have been obtained for the

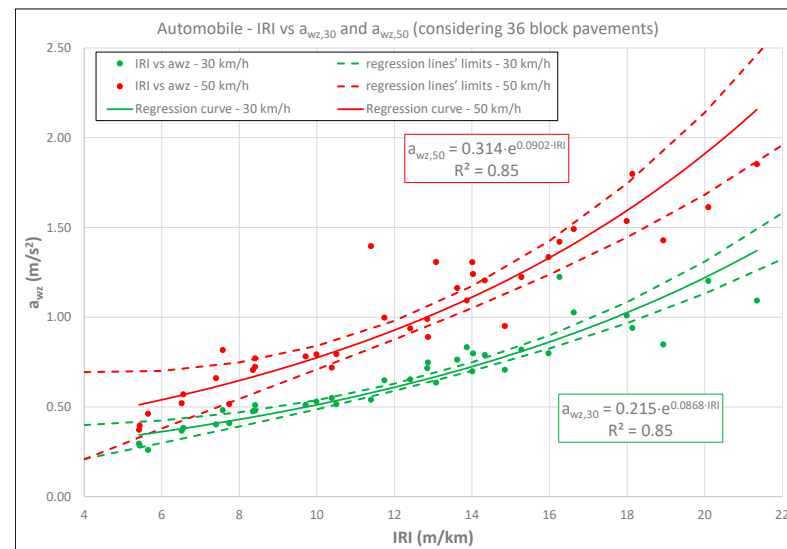
correlations between IRI and a_{wz} values with the bike models (both $a_{wz,10}$ and $a_{wz,20}$), and $a_{wz,50}$ with the bus model. Dashed lines in Figure 4a–c represent the regression lines' upper and lower limits for the individual observations [33]: they confirm that the automobile model and the bus model at 30 km/h give a_{wz} values reflecting IRI, while the confidence limits for the regression lines of the bike model and the bus model at 50 km/h are not reliable. Such different behaviors could be attributed to the effect of both the localized irregularities on a_{wz} values more than IRI and the adopted vehicle model. Therefore, IRI is not suitable to interpret the comfort for all vehicles and at all speeds.

Table 3. Calculated a_{wz} values.

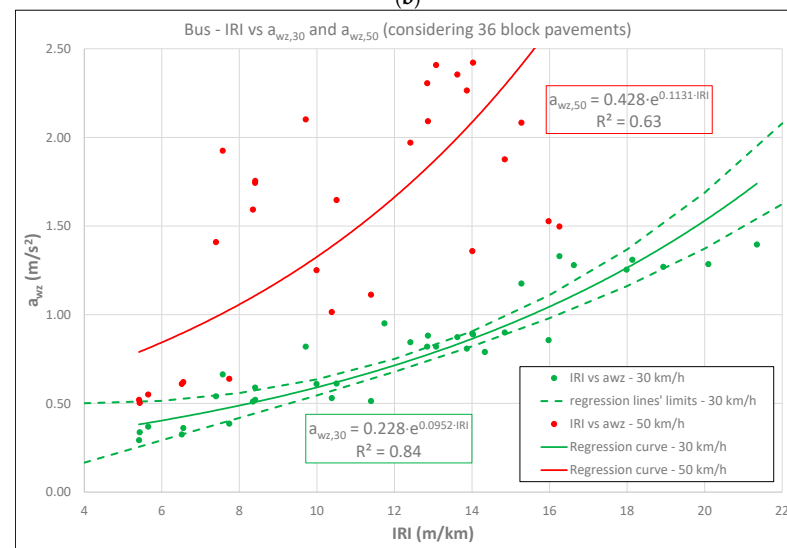
Pavement Code	Bike		Automobile		Bus	
	$a_{wz,10}$	$a_{wz,20}$	$a_{wz,30}$	$a_{wz,50}$	$a_{wz,30}$	$a_{wz,50}$
BR_1	0.86	1.18	0.75	1.18	0.88	>2.50
BR_2	2.35	2.90	1.22	1.42	1.33	>2.50
BR_3	0.82	1.23	1.40	>2.50	1.63	>2.50
BR_4	0.58	0.66	0.30	0.37	0.29	0.52
BR_5	0.55	0.78	0.48	0.71	0.51	1.59
BR_6	0.47	0.67	0.29	0.40	0.34	0.50
BR_7	0.24	0.33	0.26	0.46	0.37	0.55
BR_8	0.37	0.45	0.19	0.23	0.20	0.63
BR_9	0.66	1.03	0.58	0.97	0.80	1.35
BR_10	1.02	1.38	0.62	0.76	0.72	1.23
BR_11	0.59	0.77	0.51	0.77	0.52	1.75
BR_12	0.61	0.85	0.52	0.79	0.61	1.65
BR_13	0.56	0.78	0.54	1.40	0.51	1.11
BR_14	0.99	1.52	1.20	1.61	1.29	>2.50
BR_15	0.58	0.80	0.64	1.31	0.82	>2.50
BR_16	0.72	1.13	0.71	0.95	0.90	1.88
BR_17	0.57	0.83	0.41	0.52	0.39	0.64
BR_18	0.57	0.74	0.37	0.52	0.33	0.61
BR_19	1.12	1.55	0.83	1.09	0.81	>2.50
BR_20	0.71	1.03	0.65	0.94	0.85	1.97
BR_21	1.06	1.35	0.79	1.20	0.79	>2.50
BR_22	0.89	1.20	0.72	0.99	0.82	2.31
BR_23	0.88	1.15	0.76	1.16	0.87	2.35
BR_24	0.86	1.27	0.80	1.24	0.89	2.42
BR_25	0.63	0.86	0.55	0.72	0.53	1.02
BR_26	0.98	1.19	0.48	0.72	0.59	1.74
BR_27	0.64	0.87	0.38	0.57	0.36	0.62
BR_28	0.44	0.57	0.48	0.82	0.66	1.92
BR_29	0.88	1.19	1.03	1.49	1.28	>2.50
BR_30	1.21	1.55	0.94	1.80	1.31	>2.50
BR_31	1.34	1.65	0.82	1.22	1.18	2.08
BR_32	0.59	0.77	0.51	0.78	0.82	2.10
BR_33	1.30	1.88	1.09	1.85	1.40	>2.50
BR_34	1.15	1.56	0.70	1.31	0.89	1.36
BR_35	0.60	0.75	0.40	0.66	0.54	1.41
BR_36	0.97	1.27	0.85	1.43	1.27	>2.50
BR_37	1.11	1.69	0.80	1.33	0.86	1.53
BR_38	1.05	1.54	1.01	1.54	1.25	>2.50
BR_39	0.73	0.95	0.65	1.05	0.95	>2.50
BR_40	0.49	0.79	0.53	0.79	0.61	1.25



(a)



(b)



(c)

Figure 4. IRI- a_{wz} correlations for different vehicle models: (a) bike; (b) automobile; and (c) bus.

Figure 5 summarizes the regression curves (i.e., solid green and red lines) in Figure 4. The horizontal dotted black lines highlight the comfort classes proposed by the authors for urban block pavements (Table 2).

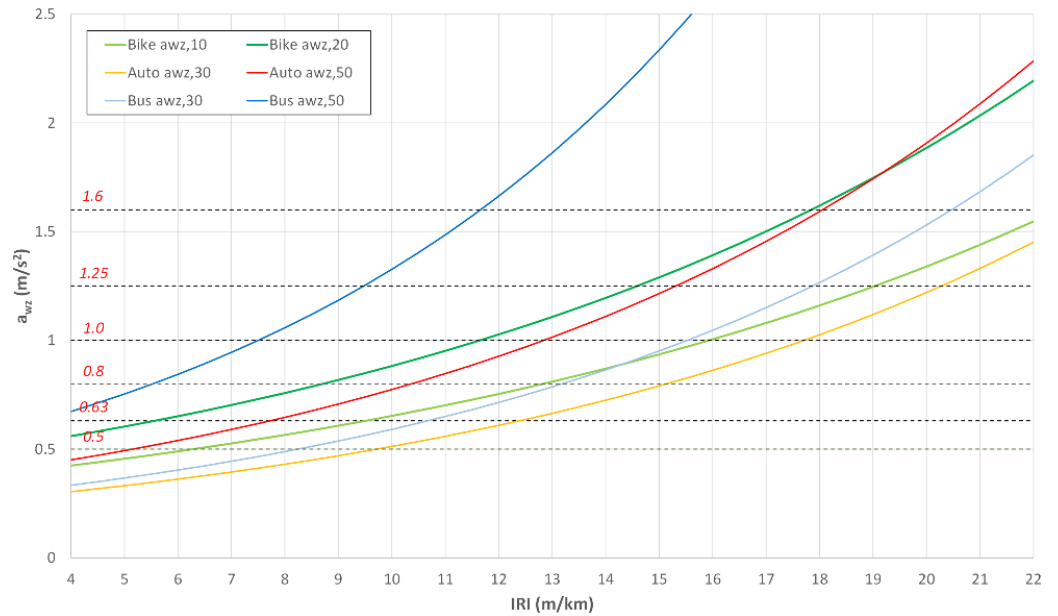


Figure 5. IRI- a_{wz} curves.

Table 4 classifies all the examined branches according to the comfort classes in Table 2. If the branch class varies with the simulated speed, the speed value in km/h is the superscript characters after the branch ID (e.g., the branch 5 belongs to Class 1 if the automobile moves at 30 km/h and to Class 2 if the automobile moves at 50 km/h). Further analyses highlighted, for example, that BR_17 and BR_33 (IRI equal to 7.74 and 21.35, and class ISO 8608 C and E, respectively) belong to Class 1 and Class 4 for all three vehicles considered. On the contrary, BR_32 (IRI equal to 9.71 and class ISO 8608 equal to C) belongs to Class 1 according to the bike model (both at 10 km/h and 20 km/h), to Class 2 according to the automobile model (both at 30 km/h and 50 km/h), and to Class 3 according to the bus model at 30 km/h. Therefore, the irregularities of BR_32 imply different comfort conditions varying the reference vehicle.

Table 4. Classification of the a_{wz} values.

Vehicle Model	Class 1 (Not uncomfortable/Little uncomfortable)	Class 2 (Little uncomfortable/Fairly uncomfortable)	Class 3 (Fairly uncomfortable)	Class 4 (Uncomfortable/Very-Extremely uncomfortable)
Bike	BR_4, BR_5, BR_6, BR_7, BR_8, BR_11, BR_12, BR_13, BR_15, BR_17, BR_18, BR_25, BR_27, BR_28, BR_32, BR_35, BR_39, BR_40	BR_1, BR_3, BR_9, BR_16, BR_20, BR_22, BR_23, BR_26, BR_29	BR_10, BR_14, BR_19, BR_21, BR_24, BR_30, BR_34, BR_36, BR_37, BR_38	BR_2, BR_31, BR_33
Automobile	BR_4, BR_5 ³⁰ , BR_6, BR_7, BR_8, BR_17, BR_18, BR_26 ³⁰ , BR_27, BR_28 ³⁰ , BR_35 ³⁰	BR_5 ⁵⁰ , BR_9 ³⁰ , BR_10, BR_11, BR_12, BR_13 ³⁰ , BR_25, BR_26 ⁵⁰ , BR_28 ⁵⁰ , BR_32, BR_35 ⁵⁰ , BR_39 ³⁰ , BR_40	BR_1, BR_9 ⁵⁰ , BR_15 ³⁰ , BR_16, BR_20, BR_21 ³⁰ , BR_22, BR_23 ³⁰ , BR_24 ³⁰ , BR_34 ³⁰ , BR_39 ⁵⁰	BR_2, BR_3, BR_13 ⁵⁰ , BR_14, BR_15 ⁵⁰ , BR_19, BR_21 ⁵⁰ , BR_23 ⁵⁰ , BR_24 ⁵⁰ , BR_29, BR_30, BR_31, BR_33, BR_34 ⁵⁰ , BR_36, BR_37, BR_38
Bus	BR_4, BR_6, BR_7, BR_8, BR_17, BR_18, BR_27	BR_5, BR_9, BR_10, BR_11, BR_12, BR_13, BR_21, BR_25, BR_26, BR_28, BR_35, BR_40	BR_1, BR_15, BR_16, BR_19, BR_20, BR_22, BR_23, BR_24, BR_32, BR_34, BR_37, BR_39	BR_2, BR_3, BR_14, BR_29, BR_30, BR_31, BR_33, BR_36, BR_38

3.3. Straightedge Analysis for Stone Pavements

Finally, the authors implemented SASP to evaluate the irregularities of stone pavements through BH curves. For each modeled vehicle and the maximum investigated speed (i.e., bike at 20 km/h; automobile and bus at 50 km/h), the pavement profiles have been investigated. In particular, the BH curves for the bike model refer to BL values between 0.25 m and 0.5 m, for the automobile model to BL values between 0.5 m and 1.5 m, and for the bus model to BL values between 1.5 m and 3 m. The comparison with the obtained a_{wz} values (Table 3) enabled us to identify for each vehicle the threshold BH curves: there are four, ranging between Class I to IV. Varying BL , the average and maximum BH values are calculated (BH_{avg} and BH_{max} , respectively) to draw the BH_{avg} and BH_{max} curves (Figure 6a,b, respectively). In Figure 6a,b, the 40 solid curves represent the BH trend of the collected pavement profiles, and their color differs for the class they belong to (i.e., green for Class I, yellow for Class II, blue for Class III, and red for Class IV). Dotted lines highlight the thresholds for each class (i.e., green for the upper boundary of Class I, blue for the upper boundary of Class II, red for the upper boundary of Class III).

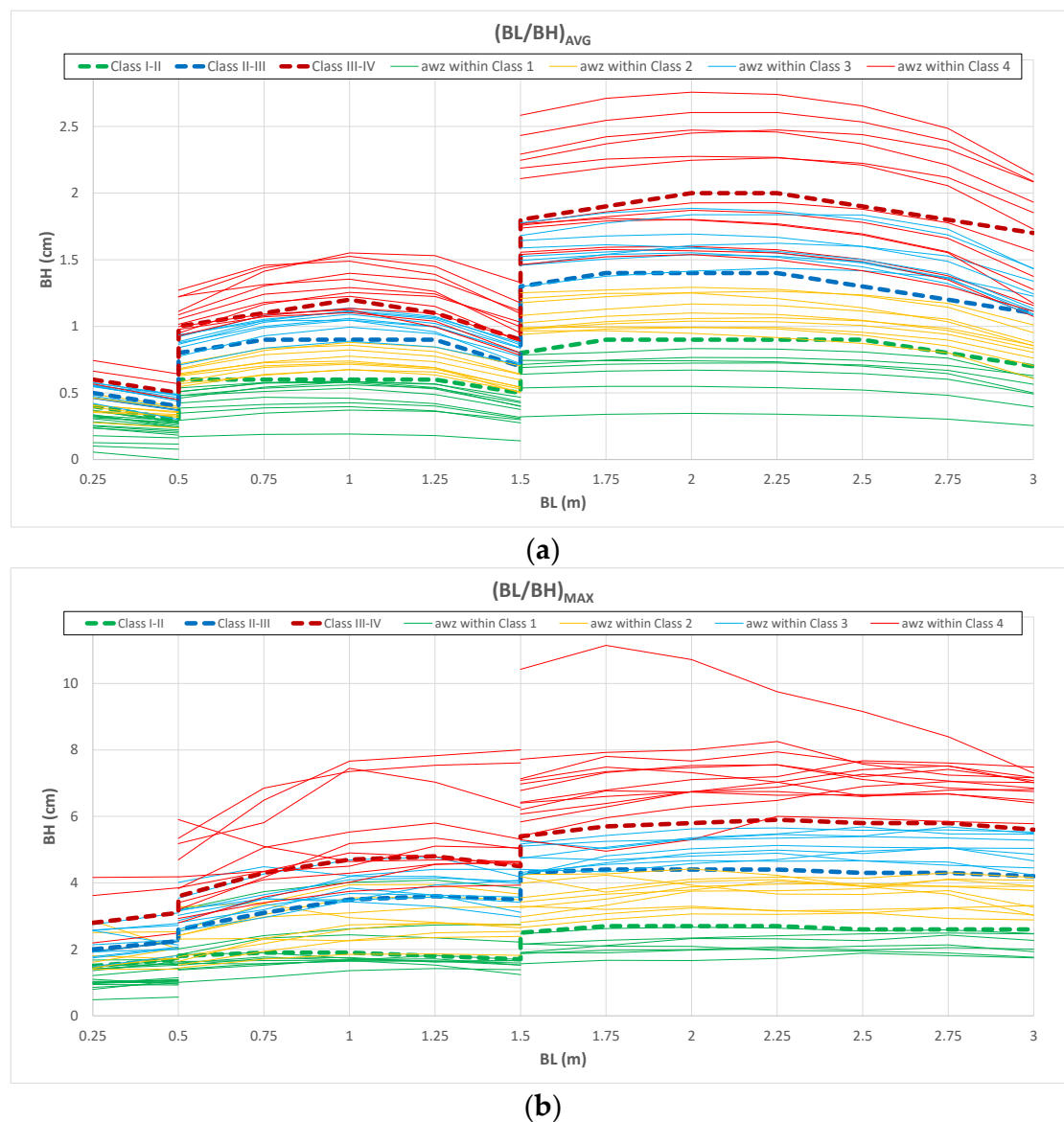


Figure 6. BH curves. (a) BH_{avg} ; (b) BH_{max} .

Figure 7a,b compare the BH curves of BR_13 (orange solid curve), BR_26 (grey solid curve), and BR_39 (green solid curve) to the threshold ones.

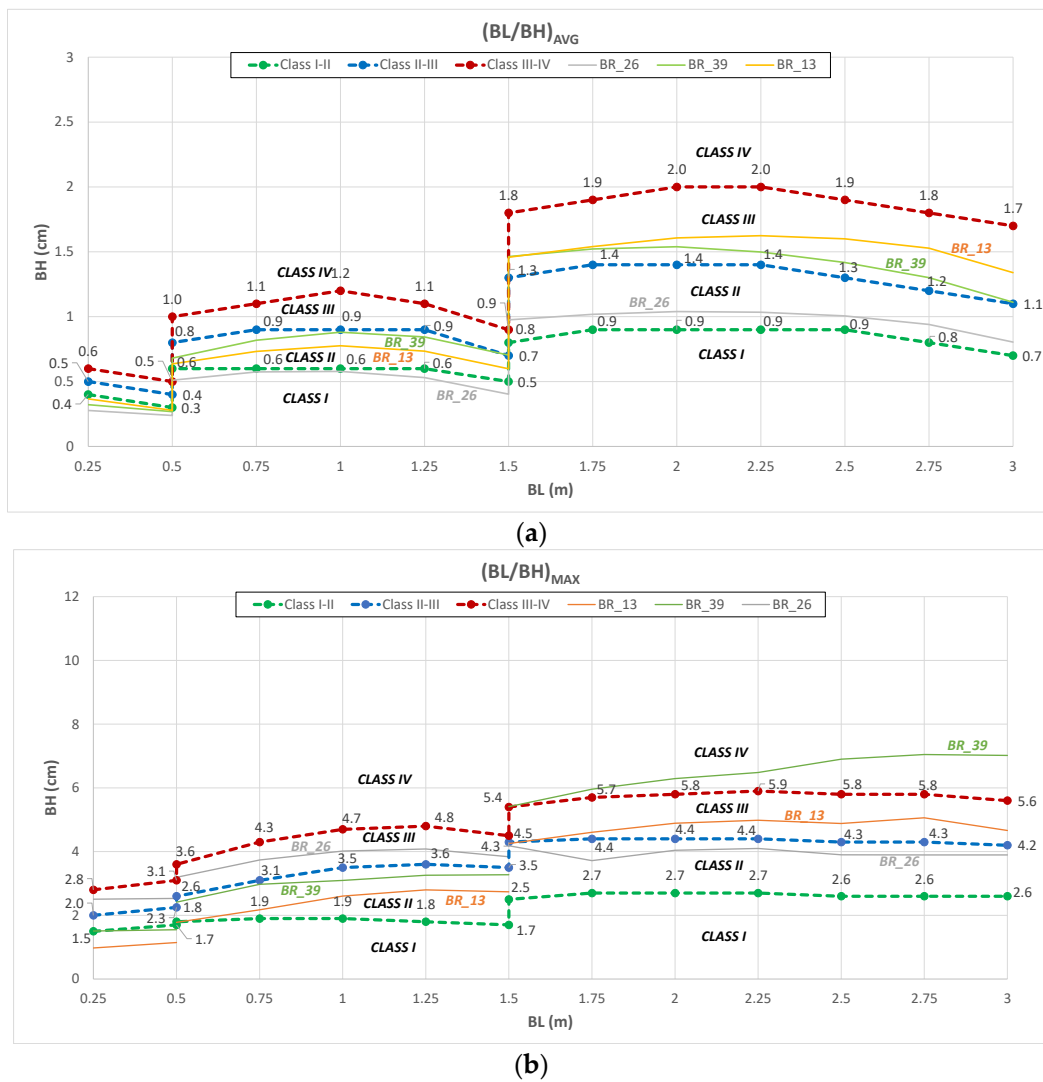


Figure 7. BH curves of BR_13, BR_26, and BR_39. (a) BH_{avg} ; (b) BH_{max} .

With regard to the bike model (i.e., BL not more than 0.5 m), in Figure 7a all the BH_{avg} curves belong to Class I, while in Figure 7b the BH_{max} curves of BR_13 and BR_39 belong to Class I and that of BR_26 belongs to Class III. With regard to the automobile model (i.e., BL between 0.5 m and 1.5 m), the BH_{avg} curve of BR_26 is in Class I, while BR_13 and BR_39 are in Class II. The classification of the latter branches is confirmed for the BH_{max} curves, while the BH_{max} curve of BR_26 belongs to Class III. With regard to the bus model (i.e., BL between 1.5 m and 3.0 m), according to the BH_{avg} criteria BR_26 is in Class II, BR_13 is in Class III, and BR_39 is in Class IV.

Table 5 lists the classification of the surveyed branches according to the proposed criteria. In particular, for each profile and vehicle model the BH_{avg} curves have been considered in order to assign the pavement to a class. Then, the identified class has been compared to that given by the corresponding BH_{max} curves: generally, the class assigned with the BH_{avg} curves is confirmed by the BH_{max} curves. Otherwise, if the class assigned with BH_{max} curves is higher than that of the BH_{avg} curves, the class from BH_{max} is assumed. It has to be noted that, in Table 5, the branches which fall into a higher class are identified by round brackets.

Table 5. Classification according to the threshold curves in Figure 6.

Vehicle Model	Class I	Class II	Class III	Class IV
Bike	BR_4, BR_5, BR_6, BR_7, BR_8, BR_11, BR_12, BR_13, BR_15, BR_17, BR_18, BR_25, BR_27, BR_28, BR_32, BR_35, BR_39, BR_40	BR_1, BR_3, BR_9, BR_16, BR_20, BR_22, BR_23, BR_(26), BR_29, BR_36	BR_10, BR_14, BR_19, BR_21, BR_24, BR_30, BR_34, BR_37, BR_38	BR_2, BR_(31), BR_33
Automobile	BR_4, BR_6, BR_7, BR_8, BR_17, BR_18, BR_27	BR_(5), BR_11, BR_12, BR_13, BR_25, BR_(26), BR_(28), BR_32, BR_(35), BR_39, BR_40	BR_1, BR_(9), BR_(10), BR_15, BR_16, BR_20, BR_21, BR_22, BR_23, BR_34	BR_2, BR_3, BR_14, BR_19, BR_(24), BR_29, BR_30, BR_31, BR_33, BR_36, BR_37, BR_38
Bus	BR_4, BR_6, BR_7, BR_8, BR_17, BR_18, BR_27	BR_5, BR_9, BR_10, BR_11, BR_12, BR_25, BR_26, BR_28, BR_35, BR_40	BR_13, BR_16, BR_20, BR_22, BR_23, BR_24, BR_32, BR_34, BR_37	BR_(1), BR_(2), BR_3, BR_14, BR_(15), BR_(19), BR_(21), BR_29, BR_30, BR_(31), BR_33, BR_36, BR_38, BR_(39)

4. Discussion

The results in Table 5 highlighted that some pavements belong to different classes when varying the vehicle model. Similar results have been obtained with regard to the a_{wz} analysis. For example, BR_5 belongs to Class I concerning bike model and Class II concerning automobile and bus models. In particular, for the automobile model, BR_5 could be in Class I with regard to BH_{avg} curves but it falls into Class II due to BH_{max} criteria. Further analyses of the road profiles showed that this evidence depends on localized irregularities such as potholes or bumps. This circumstance highlights how important it is to consider the localized irregularities in the assessment of the deterioration of the stone paving and how SASP can identify their contribution.

Table 6 presents the comparison of the results in Tables 4 and 5 and shows a substantial consistency in terms of classification (i.e., 98%, 80%, and 85% for bike, automobile, and bus, respectively). In case of disagreement between the classifications, three main causes have been identified:

- localized irregularities avoided a correct evaluation of the whole-body comfort (e.g., BR_10, BR_19, BR_26, and BR_39);
- in case two profiles were considered, irregularities and vehicle roll gave significantly different comfort results by varying the speed vehicle from 30 km/h to 50 km/h (i.e., BR_23 and BR_39);
- irregularities' wavelength affected the modeled vehicle at 50 km/h (e.g., BR_13, BR_15, and BR_21); further analyses should involve different vehicle models to investigate this issue.

Table 6. Comparison between a_{wz} and SASP results.

Code	Bike			Automobile			Bus		
	Class Table 4	Class Table 5	Comparison	Class Table 4	Class Table 5	Comparison	Class Table 4	Class Table 5	Comparison
BR_1	2	II	=	3	III	=	3	(IV)	↑
BR_2	4	IV	=	4	IV	=	4	(IV)	=
BR_3	2	II	=	4	IV	=	4	IV	=
BR_4	1	I	=	1	I	=	1	I	=
BR_5	1	I	=	1 ³⁰ -2 ⁵⁰	(II)	=	2	II	=

Table 6. Cont.

Code	Bike			Automobile			Bus		
	Class Table 4	Class Table 5	Comparison	Class Table 4	Class Table 5	Comparison	Class Table 4	Class Table 5	Comparison
BR_6	1	I	=	1	I	=	1	I	=
BR_7	1	I	=	1	I	=	1	I	=
BR_8	1	I	=	1	I	=	1	I	=
BR_9	2	II	=	2 ³⁰ -3 ⁵⁰	(III)	=	2	II	=
BR_10	3	III	=	2	(III)	↑	2	II	=
BR_11	1	I	=	2	II	=	2	II	=
BR_12	1	I	=	2	II	=	2	II	=
BR_13	1	I	=	2 ³⁰ -4 ⁵⁰	II	↓	2	III	↑
BR_14	3	III	=	4	IV	=	4	IV	=
BR_15	1	I	=	3 ³⁰ -4 ⁵⁰	III	↓	3	(IV)	↑
BR_16	2	II	=	3	III	=	3	III	=
BR_17	1	I	=	1	I	=	1	I	=
BR_18	1	I	=	1	I	=	1	I	=
BR_19	3	III	=	4	IV	=	3	(IV)	↑
BR_20	2	II	=	3	III	=	3	III	=
BR_21	3	III	=	3 ³⁰ -4 ⁵⁰	III	↓	2	(IV)	↑↑
BR_22	2	II	=	3	III	=	3	III	=
BR_23	2	II	=	3 ³⁰ -4 ⁵⁰	III	↓	3	III	=
BR_24	3	III	=	3 ³⁰ -4 ⁵⁰	(IV)	=	3	III	=
BR_25	1	I	=	2	II	=	2	II	=
BR_26	2	(II)	=	1	II	↑	2	II	=
BR_27	1	I	=	1	I	=	1	I	=
BR_28	1	I	=	1 ³⁰ -2 ⁵⁰	(II)	=	2	II	=
BR_29	2	II	=	4	IV	=	4	IV	=
BR_30	3	III	=	4	IV	=	4	IV	=
BR_31	4	(IV)	=	4	IV	=	4	(IV)	=
BR_32	1	I	=	2	II	=	3	III	=
BR_33	4	IV	=	4	IV	=	4	IV	=
BR_34	3	III	=	3 ³⁰ -4 ⁵⁰	III	↓	3	III	=
BR_35	1	I	=	1 ³⁰ -2 ⁵⁰	(II)	=	2	II	=
BR_36	3	II	↓	4	IV	=	4	IV	=
BR_37	3	III	=	4	IV	=	3	III	=
BR_38	3	III	=	4	IV	=	4	IV	=
BR_39	1	I	=	2 ³⁰ -3 ⁵⁰	II	↓	3	(IV)	↑
BR_40	1	I	=	2	II	=	2	II	=

Note: () value from BH_{max} values; the equals sign (=) denotes consistency in terms of classification according to ISO 2631 and SASP, the upward arrow (↑) denotes the SASP class is higher than that according to ISO 2631, and the downwards arrow (↓) denotes the SASP class is lower than that according to ISO 2631.

Therefore, the proposed SASP classification into I to IV classes can be used for the prioritization of maintenance work, taking into account the expected traffic conditions.

Given the results in Tables 1 and 3–5, the proposed classes I to IV could be related to the discussed methods as follows:

- Class I: Block pavement in excellent condition which corresponds to a perfectly made surface. There are no localized irregularities larger than those of the average irregularities of the pavement. On these surfaces, circulation is guaranteed in conditions of adequate comfort up to a speed of 50 km/h for users of automobiles and buses, and up to 20 km/h for those of bikes. The reference values of the traditional performance indicators are also reported: IRI < 6–8 m/km, ISO 8608 classification “C” with values of parameters n_0 up to 300 and $w < -2.0$);
- Class II: Block pavement in acceptable conditions which corresponds to a surface with minimal localized surface defects not visible to the naked eye. On these surfaces, circulation is guaranteed in conditions of adequate comfort up to 30 km/h for automobiles and buses. For motor vehicles at 50 km/h, the a_{wz} results show fairly uncomfortable conditions due to localized irregularities that require restoration works. For bike users, the comfort conditions are still perceived as adequate up to 20 km/h depending on the trajectory travelled. The reference values of the traditional indicators are also reported: IRI = 8–10 m/km, ISO 8608 classification “C” and “D” with values of parameters $n_0 < 700$ and $w < -2.2$ – -2.4);
- Class III: Block pavement in rather degraded conditions with widespread and localized irregularities that cause fairly uncomfortable conditions at the typical urban speeds. The conditions could be uncomfortable for automobile users at 50 km/h and for buses. Therefore, restoration works should be planned shortly, to resolve both localized deterioration and widespread defects in the most critical sections. For bike users, the comfort conditions are still perceived as adequate up to 10 km/h, while for higher speeds they fall into fairly uncomfortable or uncomfortable conditions. The reference values of the traditional indicators are also reported: IRI = 10–13 m/km, ISO 8608 classification “D” with values of parameters $n_0 < 1400$ and $w < -2.3$ – -2.6);
- Class IV: Block pavement in very degraded condition with diffuse and punctual irregularities that are visible to the naked eye. Circulation is guaranteed in fairly comfortable conditions only up to 20 km/h for cars and buses. Very/extremely and uncomfortable conditions are already experienced by the users of automobiles and buses at 30 km/h, and therefore the circulation of vehicles is not recommended in such situations. For bike users, uncomfortable/very uncomfortable conditions are already perceived at 10 km/h, resulting in natural speed reductions that could lead to loss of balance for less experienced users. Therefore, the restoration works should be urgently planned. The reference values of the traditional indicators are also reported: IRI > 13 m/km, ISO 8608 classification “D” and “E” with values of parameters $n_0 > 1400$ and $w < -2.4$ – -2.8).

However, the values of the traditional indicators provided for each I to IV class may be considered as reference and not mandatory. Indeed, only SASP ranks the pavement profiles for different vehicle categories. This feature is confirmed by the results of BR_14 whose IRI value and ISO 8608 classification would place it in Class IV, while it falls into Class II for $a_{wz,10}$ and Class III for $a_{wz,20}$ referring to the bikes.

SASP was conceived for assessing the irregularities of stone pavements, but it can be applied to all types of modular pavements. Indeed, the study investigated road surfaces paved with different materials and layout. Possible future developments could concern the proposal of automated methodologies for the extraction of true profiles from 3D surface surveys of the pavement carried out using lidar instrumentation [34]. Moreover, further applications could be the identification of localized irregularities on asphalt pavements and the proposal of new thresholds.

5. Conclusions

In this two-part paper, four methods for assessing irregularities of stone pavements have been critically examined with reference to an extensive sample of profile measurements. The examined traditional methods (i.e., the International Roughness Index, the surface profile classification according to ISO 8608, and the comfort index according to ISO 2631) are designed for continuous pavements and do not provide thresholds to set the road operating conditions and schedule proper maintenance activities for modular pavements. On the other hand, the authors proposed SASP in order to identify localized irregularities on stone pavements and provide serviceability limits for different urban vehicles. In particular, it is based on the measurement of real profiles of the pavement and considers bikes, automobiles, and buses to assess the proper pavement degradation level. Four classes have been defined, varying from Class I (i.e., perfect geometric conditions and adequate comfort conditions) to Class IV (degraded road surfaces and extreme discomfort conditions). The defined classes domain is based on *BH* curves, and they agreed with the results from the other methods for each vehicle. It has to be noted that the compared methods differ for the approach (geometric or comfort based) and return not-overlapping results: 40 branch profiles have been collected through a contact profilometer and the results are:

- 32 branch profiles have IRI values higher than 8 m/km (a typical limit to define bad pavement conditions).
- The classification according to ISO 8608 [13] identify six branch profiles in Class E (destroyed roads belong to classes above D) and 0 profiles in Class A.
- The comfort classification according to ISO 2631 [14] identifies, for bikes, 18 branches in Class 1 and 3 in Class 4; for automobiles 11 branches in Class 1 and 17 in Class 4; and for buses 7 branches in Class 1 and 10 in Class 4;
- SASP identifies, for bikes, 18 branches in Class I and 3 branches in Class IV; for automobiles 7 branches in Class I and 12 in Class IV; and for buses 7 branches in Class I and 14 in Class IV.

The SASP classification proposed for stone pavements showed good agreement with the ISO 2631 comfort classification with regard to three different road vehicles; in particular, the results matched for bikes in 39 cases out of 40, for automobiles in 32 cases out of 40, and for buses in 35 cases out of 40. For each proposed class, a comparative analysis with traditional roughness evaluation methods has been carried out. For example, less than 8 m/km IRI values stand for Class I, 8–10 m/km IRI values for Class II, 10–13 m/km IRI values for Class III, and more than 13 m/km IRI values for Class IV. Similarly, for each of the four defined stone paving classes, the values of the parameters n_0 and w were identified to generate artificial road profiles and investigate them according to ISO 8608.

Therefore, the novel method allows the urban road manager to classify the network of stone pavements by prioritizing the interventions of greater historical and artistic value and which manifest the most critical situations with respect to the comfort of users. Further developments consist of the implementation of SASP to non-stone modular and flexible pavements.

Author Contributions: Conceptualization, S.B. and G.L.; data curation, G.C., P.D.M. and L.M.; formal analysis, G.L.; funding acquisition, A.D.; investigation, G.L.; methodology, G.C. and G.L.; project administration, G.L. and P.D.M.; resources, A.D. and P.D.M.; software, S.B. and G.L.; supervision, G.C. and A.D.; validation, A.D., P.D.M. and L.M.; visualization, L.M.; writing—original draft, G.L.; writing—review and editing, G.L., P.D.M. and L.M. All authors have read and agreed to the published version of the manuscript.

Funding: This research was developed within the PRIN 2017 “Stone pavements. History, conservation, valorisation and design” (20174JW7ZL) financed by the Ministry of Education, University and Research (MIUR) of the Italian Government and within the grant number RM120172B05C0B39, title “Urban pavement monitoring system using car and bike/scooter sharing vehicles”, financed by the Sapienza, University of Rome.

Institutional Review Board Statement: Not applicable.

Informed Consent Statement: Not applicable.

Data Availability Statement: Not applicable.

Acknowledgments: The authors thank Eng. Cristiano Fustaino and we acknowledge his work. Fustaino surveyed and collected the measurements on the pavements, and he applied the software implemented by the authors for the irregularities assessment.

Conflicts of Interest: The authors declare no conflict of interest. The funders had no role in the design of the study; in the collection, analyses, or interpretation of data; in the writing of the manuscript; or in the decision to publish the results.

References

- Kim, I.-J. Safety Assessment of the Community Facilities for the Prevention of Pedestrian Fall Incidents: Concrete Footpaths and Walkways. *J. Perform. Constr. Facil.* **2022**, *36*, 04022061. [\[CrossRef\]](#)
- Fini, A.; Frangi, P.; Comin, S.; Vigevani, I.; Rettori, A.A.; Brunetti, C.; Moura, B.B.; Ferrini, F. Effects of pavements on established urban trees: Growth, physiology, ecosystem services and disservices. *Landsc. Urban Plan.* **2022**, *226*, 104501. [\[CrossRef\]](#)
- Zoccali, P.; Moretti, L.; Di Mascio, P.; Loprencipe, G.; D'Andrea, A.; Bonin, G.; Teltayev, B.; Caro, S. Analysis of natural stone block pavements in urban shared areas. *Case Stud. Constr. Mater.* **2018**, *8*, 498–506. [\[CrossRef\]](#)
- Garilli, E.; Autelitano, F.; Giuliani, F. A study for the understanding of the Roman pavement design criteria. *J. Cult. Herit.* **2017**, *25*, 87–93. [\[CrossRef\]](#)
- Garilli, E.; Giuliani, F. Stone pavement materials and construction methods in Europe and North America between the 19th and 20th century. *Int. J. Arch. Herit.* **2019**, *13*, 742–768. [\[CrossRef\]](#)
- Loprencipe, G.; Di Mascio, P.; Moretti, L.; Zoccali, P. Analytical and Numerical Approaches for Design of Stone Pavers in Urban Shared Areas. *IOP Conf. Ser. Mater. Sci. Eng.* **2019**, *471*, 062030. [\[CrossRef\]](#)
- Garilli, E.; Bruno, N.; Autelitano, F.; Roncella, R.; Giuliani, F. Automatic detection of stone pavement's pattern based on UAV photogrammetry. *Autom. Constr.* **2020**, *122*, 103477. [\[CrossRef\]](#)
- Zoccali, P.; Loprencipe, G.; Galoni, A. Sampietrini Stone Pavements: Distress Analysis Using Pavement Condition Index Method. *Appl. Sci.* **2017**, *7*, 669. [\[CrossRef\]](#)
- Moretti, L.; Di Mascio, P.; Loprencipe, G.; Zoccali, P. Theoretical analysis of stone pavers in pedestrian areas. *Transp. Res. Procedia* **2020**, *45*, 169–176. [\[CrossRef\]](#)
- Bruno, S.; Del Serrone, G.; Di Mascio, P.; Loprencipe, G.; Ricci, E.; Moretti, L. Technical proposal for monitoring thermal and mechanical stresses of a runway pavement. *Sensors* **2021**, *21*, 6797. [\[CrossRef\]](#)
- Garilli, E.; Autelitano, F.; Freddi, F.; Giuliani, F. Urban pedestrian stone pavements: Measuring functional and safety requirements. *Int. J. Pavement Eng.* **2021**, *23*, 4748–4759. [\[CrossRef\]](#)
- Peraka, N.S.P.; Biligiri, K.P. Pavement asset management systems and technologies: A review. *Autom. Constr.* **2020**, *119*, 103336. [\[CrossRef\]](#)
- ISO 8608; Mechanical Vibration—Road Surface Profiles—Reporting of Measured Data. International Organization for Standardization: Geneva, Switzerland, 2016.
- ISO 2631-1; Mechanical Vibration and Shock-Evaluation of Human Exposure to Whole-Body Vibration. International Organization for Standardization: Geneva, Switzerland, 1997.
- FAA. *Guidelines and Procedures for Measuring Airfield Pavement Roughness*; FAA: Washington, DC, USA, 2014.
- Loprencipe, G.; Bruno, S.; Cantisani, G.; D'Andrea, A.; Di Mascio, P.; Moretti, L. Methods for Measuring and Assessing Irregularities of Stone Pavements—Part I. *Sustainability* **2023**, *15*, 1528. [\[CrossRef\]](#)
- Loprencipe, G.; Zoccali, P. Comparison of methods for evaluating airport pavement roughness. *Int. J. Pavement Eng.* **2019**, *20*, 782–791. [\[CrossRef\]](#)
- Soffarina, M.S.S. Mountain Bicycle Cycling Comfort on Different Road Surfaces. *J. Sci. Appl. Eng.* **2020**, *3*, 29–34. [\[CrossRef\]](#)
- Thigpen, C.G.; Li, H.; Handy, S.L.; Harvey, J. Modeling the impact of pavement roughness on bicycle ride quality. *Transp. Res. Rec.* **2015**, *2520*, 67–77. [\[CrossRef\]](#)
- Tong, Z.; Gao, J.; Sha, A.; Hu, L.; Jiang, W.; Huang, Y. Evaluating the cycling comfort on urban roads based on cyclists' perception of vibration. *J. Clean. Prod.* **2018**, *192*, 531–541.
- Nguyen, T.; Lechner, B.; Wong, Y.D.; Tan, J.Y. Bus Ride Index—a refined approach to evaluating road surface irregularities. *Road Mater. Pavement Des.* **2021**, *22*, 423–443. [\[CrossRef\]](#)
- Wu, R.; Louw, S.; Li, H.; Harvey, J.T.; Thigpen, C. Bicycle Vibration and Pavement Ride Quality for Cyclists. In Proceedings of the 94th Annual Meeting of the Transportation Research Board, Washington, DC, USA, 11–15 January 2015.
- Sidhant, V.K. Bicycle Ride Comfort Evaluation and Optimization. Master's Thesis, University of Pretoria, Pretoria, South Africa, 2019.
- Huang, J.; Fournier, N.; Skabardonis, A. Bicycle level of service: Proposed updated pavement quality index. *Transp. Res. Rec.* **2021**, *2675*, 1346–1356. [\[CrossRef\]](#)

25. Sekulić, D.; Dedović, V.; Rusov, S.; Šalinić, S.; Obradović, A. Analysis of vibration effects on the comfort of intercity bus users by oscillatory model with ten degrees of freedom. *Appl. Math. Model.* **2013**, *37*, 8629–8644. [[CrossRef](#)]
26. Gogola, M. Analysing the vibration of bicycles on various road surfaces in the city of Žilina. *Arch. Motoryz.* **2020**, *88*, 77–97. [[CrossRef](#)]
27. The-Face[®]-Companies Dipstick[®] Norfolk, VA 23508. Available online: <https://facecompanies.com/dipstick/> (accessed on 6 February 2023).
28. ASTM E1926-08; Standard Practice for Computing International Roughness Index of Roads from Longitudinal Profile Measurements. ASTM International: West Conshohocken, PA, USA, 2015.
29. Bruno, S.; Vita, L.; Loprencipe, G. Development of a GIS-Based Methodology for the Management of Stone Pavements Using Low-Cost Sensors. *Sensors* **2022**, *22*, 6560. [[CrossRef](#)] [[PubMed](#)]
30. Hanusz, Z.; Tarasinska, J.; Zielinski, W. Shapiro–Wilk test with known mean. *Revstat Stat. J.* **2016**, *14*, 89–100.
31. Cantisani, G.; Loprencipe, G. Road Roughness and Whole Body Vibration: Evaluation Tools and Comfort Limits. *J. Transp. Eng.* **2010**, *136*, 818–826. [[CrossRef](#)]
32. Mucka, P. Simulated Road Profiles According to ISO 8608 in Vibration Analysis. *J. Test. Eval.* **2018**, *46*, 405–418.
33. Loprencipe, G.; Moretti, L.; Pantuso, A.; Banfi, E. Raised Pedestrian Crossings: Analysis of Their Characteristics on a Road Network and Geometric Sizing Proposal. *Appl. Sci.* **2019**, *9*, 2844. [[CrossRef](#)]
34. De Blasiis, M.R.; Di Benedetto, A.; Fiani, M. Mobile Laser Scanning Data for the Evaluation of Pavement Surface Distress. *Remote Sens.* **2020**, *12*, 942. [[CrossRef](#)]

Disclaimer/Publisher’s Note: The statements, opinions and data contained in all publications are solely those of the individual author(s) and contributor(s) and not of MDPI and/or the editor(s). MDPI and/or the editor(s) disclaim responsibility for any injury to people or property resulting from any ideas, methods, instructions or products referred to in the content.